INTERFACE SCIENCE 11, 199–209, 2003

Effect of Interfaces on the Crystallization Behavior of PDMS

T. DOLLASE*, M. WILHELM AND H.W. SPIESS
Max-Planck-Institut für Polymerforschung, Ackermannweg 10, 55128 Mainz, Germany

Y. YAGEN, R. YERUSHALMI-ROZEN† AND M. GOTTLIEB
Department of Chemical Engineering, Ben-Gurion-University of the Negev, Beer-Sheva 84105, Israel; The Reimund Stadler Minerva Center for Mesoscale Macromolecular Engineering, Ben-Gurion-University of the Negev, Beer-Sheva 84105, Israel
rachely@bgumail.bgu.ac.il

Abstract. The reversible thermal behavior of a non-entangled semicrystalline polymer, poly(dimethylsiloxane), PDMS, was investigated in the presence of sub-micron particles. Filled polymer systems of this type are characterized by a large surface-to-volume ratio but lack the external confinement that is typical for a thin film geometry. Differential-scanning calorimetry (DSC) measurements indicate that the presence of the nanometric solid additives enhances the crystallization rate as compared to native PDMS melts. Different types of additives and surface interactions resulted in a similar effect, suggesting that the origin of the enhanced crystallinity is non-specific. The effect is attributed to entropic interactions in the boundary layer.

Keywords: polymer crystallization, surface effects in polymers

1. Introduction

Surfaces are known to affect the physical properties of polymers and modify their dynamic behavior [1–7]. In particular, first order thermal transitions (crystallization or melting) and second order relaxation processes (glass formation) of polymers deviate significantly in the vicinity of a surface from their bulk behavior [8–11].

Most polymers form amorphous solids as crystallization requires extensive regularity on a chemical (e.g., tacticity) and topological (branching, crosslinking) level. In a crystallizable polymer, the degree of crystallinity is limited by the presence of topological constraints and disparity in chain lengths. The class of polymers that embodies crystalline domains is known as semi-crystalline polymers [12]. The degree of crystallinty as well as the crystal habit: Structure, size and orientation of the crystals, affect bulk properties of the polymeric materials, and are therefore important parameters for most applications [13].

Polymer crystallization from the melt involves ordering at different length scales: It is often observed that aggregates of crystals, originating from a common center, form spherulites (Fig. 1(a)). Each of the crystallites is constructed of lamellar layers (Fig. 1(b)), formed by chain folding along the short direction of the layer. Chain folding is the essential step in the transformation of a polymer liquid (the melt) into a crystal.

Along the normal to the lamellar layer crystalline and amorphous regions alternate. The amorphous regions incorporate chain entanglements, branches, side-chains, and chain ends.

When crystallization is induced by cooling of a high molecular-weight polymer melt at a finite rate, the ideal crystalline structure can not be realized, due to the typically slow dynamics of polymer re-organization

*Present address: Tesa AG, Quickbornstrasse 24, 20253 Hamburg, Germany.
†To whom all correspondence should be addressed.

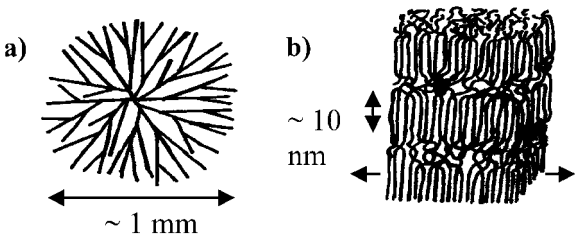

Figure 1. A schematic drawing of polymeric crystallites on two different length scales. (a) Spherulites—the diameter of fully developed spherulites ranges from several microns to centimeters. Throughout the spherulite amorphous (white) and crystalline (black) regions alternate. (b) Typical lamellar structure. The thickness is in the order of 10 nm.

and topological constraints. The latter is often much longer than the experimental time-scale. As a consequence, the structures that develop at a given temperature, and a given cooling rate, are the fastest ones to assemble and grow, rather than those of the lowest free energy. Being dominantly controlled by kinetics, structure, properties, and the degree of crystallinity, are affected by the crystallization temperature, cooling rate, and last, but not-least, the initial conformational state of the chains [12].[1]

Classical theories of polymer crystallization such as the Hoffman-Lauritzen model [14, 15], describe the process as a sequence of two steps: Primary nucleation and growth, with nucleation being the rate-determining step [16]. Nucleation is classified as either homogeneous [17] or heterogeneous. Crystal growth takes place by piecewise incorporation of macromolecular chains on a pre-existing crystal surface, known as secondary nucleation [15].

A different model for the growth mechanism of crystals was suggested by Sadler [18]: In his model the elementary step leading to crystallization is reversible attachment and detachment of chain sequences. The model suggests that the growth process evolves by natural selection of the configurations which lead to growth of the crystalline face. Both models assume that the lamellar crystallites grow into the melt, and there exists a well-defined interface between the ordered phase and the melt, in a similar manner to crystallization of small molecules.

A conceptually different model was recently described by Strobl and coworkers [19, 20]. They suggested that in some cases, polymer crystallization from the melt evolves by cooperative ordering over large regions. Here mesoscopic domains of preordered molten chains separate regions of crystalline and non-oriented molten material. In this approach crystallization is viewed as a disorder-order transition, similar to that observed in two-dimensional monolayers [21]. The process involves the formation of a novel phase referred to as granular crystalline phase characterized by local ordering. It should be noted that the concept of weakly ordered phases was discussed in the context of linear chains crystallization (see for example ref. 22).

The effect of solid micro-particles such as dispersed granular filler on polymer crystallization was investigated in a considerable number of calorimetric studies [13]. It was observed that the presence of particles affect the resulting crystallite size, degree of crystallinity as well as crystallization temperature, T_c, and melting temperature, T_m [23]. These observations are of technical importance in the field of composites and reinforced materials.

In the framework of the classical models of crystallization it was suggested that solid surfaces enhance crystallinity by locally reducing the critical enthalpy for nucleation, an effect known as heterogeneous nucleation [16]. Yet many of the observations cannot be explained by a local reduction of enthalpy.

In the study described here we examine the effect of surfaces on the calorimetric response of a practically non-entangled semicrystalline polymer, poly(dimethylsiloxane), PDMS [24]. Particles are dispersed in a melt, therefore exhibit a large surface-to-volume ratio which emphasizes the effect of interfacial interactions. Yet, unlike a thin-film configuration, finite size and external confinement do not play a dominant role in this system. The experiments monitor the crystallization and glass-transition characteristics in the presence of four different types of interfaces, some of which are enthalpically attractive. Thus, we are able to examine the specific and general aspects of the interfacial interaction, in the context of PDMS crystallization.

The structure of the article is as follows: We describe the preparation and characterization of the samples, introduce the experimental technique, discuss the results and compare them with theoretical predictions.

2. Experimental Section

Materials and Sample Preparation: PDMS from three different sources was used: PDMS 16,000 g mol^{-1} (PDMS 16k) was synthesized by living ring-opening polymerization by T. Wagner at the Max-Planck-Institut für Polymerforschung, Mainz, Germany.

PDMS 15,000 g mol^{-1} (PDMS 15k) was purchased from Polymer Source, Dorval, Canada and PDMS 8,850 g mol^{-1} (PDMS 8.8k) was purchased from PSS Germany (we report all molecular weight data in terms of the number average, M_n; the polydispersity of all polymers was $M_w/M_n = 1.1$, determined by GPC). These molecular weights are roughly of the order of the entanglement length, M_e, of PDMS and we regard PDMS 16k as practically non-entangled.[2]

Fumed silica Cab-o-Sil M7D particles (Cabot Corp., Boston, U.S.A.) were used. These particles form three-dimensional aggregates of an average size of 250 nm consisting of individual particles of 10–20 nm in diameter and with a surface area of 200 ± 25 m^2 g^{-1}. The silica aggregates were employed with three different modifications: (a) as dried particles, (b) saturated with water (c) dried and coated by a fluorinated silane. The first type of particles was dried by heating at 200°C *in vacuo* for 24 hours. Loss of water was monitored by the decrease in the intensity of the water band at 3440 cm^{-1} using FTIR spectroscopy. Fluorination was carried out by immersion of pre-dried particles for 3 hours at ambient temperature in a solution (90% isooctane, Merck, 10% choroform, Frutarom, both HPLC grade) of 1H,1H,2H,2H-perfluorodecyltrichlorosilane, PFDTS (Lancaster). The solvent was then evaporated and the particles were rinsed in chloroform, filtered and dried at 100°C *in vacuo* over night. Surface coverage was estimated from FTIR measurements which were carried out by mixing 5 mg of particles in 100 mg of KBr. The IR spectra of the coated particles exhibited three extra bands at 650, 700 and 900 cm^{-1} corresponding to C-F bending vibrations and additionally a characteristic band slightly below 3000 cm^{-1} revealing C-H stretching modes. No peak was observed at 3440 cm^{-1} indicating the absence of water on the particle surface. PDMS does not wet a surface coated with PFDTS and forms a contact angle of $45^\circ \pm 1$ (advancing) and $35^\circ \pm 1$ (receding).

Controlled Porous Glass (CPG) [25, 26] was purchased from Schott, Hofheim, Germany, in a hydrophilic and hydrophobic form. The hydrophilic glass is a powder of borosilicate which carries Si-OH groups on the surface. In the hydrophobic glass 25% of the OH-groups are exchanged by $C_8H_{17}O$-groups. Both materials are characterized by an average particle size of 30–60 μm and an average pore size of about 100 nm.

The filled polymer mixtures were prepared by stirring of the filler particles in a solution of PDMS in heptane (HPLC grade, Aldrich) for at least 5 hours at ambient temperature. The solvent was then evaporated and the suspension was dried for 24 hours at 85°C. In this study we used a particle concentration of 10 wt% in PDMS. The distribution of the filler particles in the polymeric matrix was characterized by freeze-fracture transmission-electron microscopy (FFTEM). Samples were prepared by placing a filled polymer melt between two copper disks and vitrifying the sample by plunging it into liquid propane, cooled by liquid nitrogen. A Balzers BAF 400 freeze-fracture apparatus was used for fracturing and replication at about 130 K. For electron microscopy Pt/C was deposited at an angle of 45°. The PDMS was removed from the replica using a 1:1 (v/v) mixture of THF and methanol. The clean replica was then imaged in a CEM 902 transmission-electron microscope. In Fig. 2 we present typical images of water-saturated M7D particles dispersed in PDMS 15k. We observe that the particles are well dispersed, and that the inter-aggregate distance is of the order of 1 μm.

Experimental Technique: Differential-scanning calorimetry (DSC) served as the main experimental tool in this study. This is a thermoanalytical technique that records heat flux changes as a function of time [27, 28]. First-order phase transitions like melting or crystallization appear in the thermogram as peaks while a glass transition shows up as a step. In this study we performed experiments at constant rates where the sample was nominally cooled or heated at a constant rate, β ($dT/dt = \beta = \text{constant}$, where T is temperature and t is time). Unless stated otherwise the cooling rate was $\beta = -5$ K min^{-1} and the heating rate $\beta = +5$ K min^{-1}. The experiments were performed in a Mettler Toledo Thermal Analysis System TA 8000, equipped with a DSC 820 module hooked up to a liquid N_2 cooling device. Purge gas was dry N_2 (80 ml min^{-1}). Melting temperature and enthalpy of fusion calibration were carried out using indium (Mettler) and heptane (HPLC grade, Aldrich). We report glass-transition temperatures as midpoints and first-order phase transition temperatures as peak temperatures. All data are normalized with respect to the mass of PDMS and for β when required.

3. Results

A thermogram of pure PDMS 15k including cooling and heating scans is shown in Fig. 3(a), and the numerical data are presented in Table 1. The cooling curve reveals a small and broad exothermal crystallization peak at −88.9°C and a baseline offset at

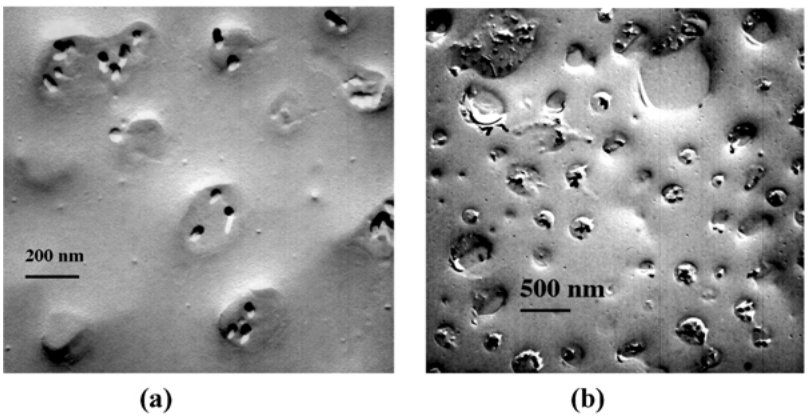

Figure 2. Freeze-fracture TEM micrographs of a sample containing 10 wt% of water-saturated M7D at two different magnifications. (a) M7D particles with an effective size of ∼250 nm constist of aggregates of smaller native particles (∼20 nm). (b) Indication of a random dispersion of M7D particles in PDMS. The measurements were carried out by Prof. Oren Regev and Mr. Klaus Horbaschek in the laboratory of Prof. Heinz Hoffmann at Bayreuth University.

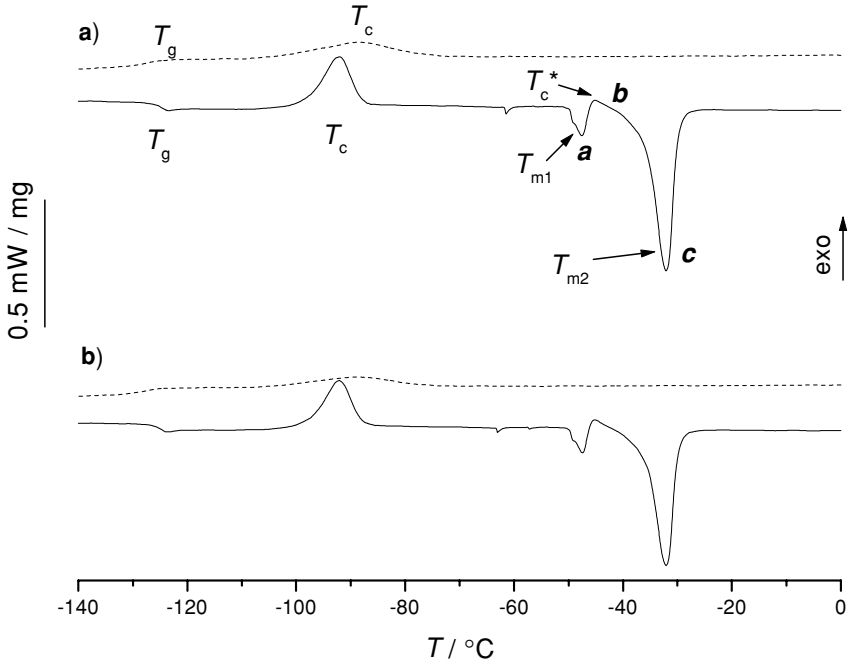

Figure 3. DSC thermogram of pure PDMS 15k. Dashed line is a cooling curve, solid line is a heating curve: (a) first run, (b) subsequent second run. In the cooling curve we observe an exothermal peak T_c and a glass transition at T_g. In the heating curve we observe a glass transition, T_g, an exothermic peak, the so-called cold crystallization, T_c, two melting peaks, T_{m1} (***a***) and T_{m2} (***c***), and a recrystallization exotherm, T_c^* (***b***). Numerical values are given in Table 1.

−125.0°C that is due to a glass transition. In the heating curve we observe, T_g, and a narrow and relatively large exothermic peak, the so-called cold crystallization, T_c, at −92.3°C. At yet higher temperatures we detect two melting peaks, labelled (***a***) and (***c***) in Fig. 3(a) and an additional crystallization exotherm, (***b***), at −45.2°C situated just between the two melting peaks. This is in agreement with previous studies of PDMS [29–33]. At the given cooling rate of $-5\ \mathrm{K\ min^{-1}}$ the crystallization of PDMS is almost completely quenched as indicated by the very small crystallization exotherm observed during the cooling scan and most of the crystallizable

Table 1. Thermal data for non-filled PDMS obtained by DSC at a cooling rate of -5 K min^{-1} and a heating rate of $+5$ K min^{-1}. Data are given for two subsequent runs to show reproducibility.

	1st cooling	2nd cooling
T_c	$-88.9°C$	$-87.8°C$
T_g	$-125.0°C$	$-124.6°C$
	1st heating	2nd heating
T_g	$-128.0°C$	$-128.0°C$
T_c	$-92.3°C$	$-92.2°C$
T_{m1}	$-47.5°C$	$-47.4°C$
T_c*	$-45.2°C$	$-45.3°C$
T_{m2}	$-32.1°C$	$-32.1°C$

material solidifies to form an amorphous glass. In the heating scan a step in the baseline is observed which indicates a glass transition. The now fluid material is in a supercooled state and eventually the viscosity becomes low enough that chains can rearrange to form crystallites. This phenomenon is observed as cold crystallization at T_c. The resulting crystallites melt during a complex melting pattern [34 and references therein]. In Fig. 3(b) we present a subsequent measurement of the very same sample, following the cooling and heating sequence described above. We observe that the second thermogram is almost identical to the first, indicating reproducibility and the absence of memory effects and hysteresis. The thermograms presented in Fig. 3 and the experimental conditions under which the experiments were performed serve as the reference for the investigation of the particle-filled PDMS systems described below.

A thermogram of PDMS filled with 10 wt% non-dried M7D particles is presented in Fig. 4(a) and of PDMS filled with 10% dried M7D particles in Fig. 4(b) (data given in Table 2). The first significant observation in the DSC curves is the appearance of a sharp exotherm in the cooling scan. This feature is attributed to induced crystallization since the subsequent heating scan does not reveal a glass transition nor a cold crystallization peak but exhibits melting endotherms. We may therefore conclude that in this system crystallites form already during the cooling scan. The loss of the glass transition in the heating scan by itself is not a sufficient indication for a high degree of crystallization during the cooling curve: The initial calorimetric value of the step-like T_g feature is rather low and broadening can easily push it down below the detection limit of the calorimeter. The subsequent cold crystallization exotherm (or its absence) is much easier to monitor and evaluate. In addition, the crystallization exotherm is easily detected during the cooling scan. Hence, both cooling and heating scans have to be evaluated in order to obtain a complete thermal picture.

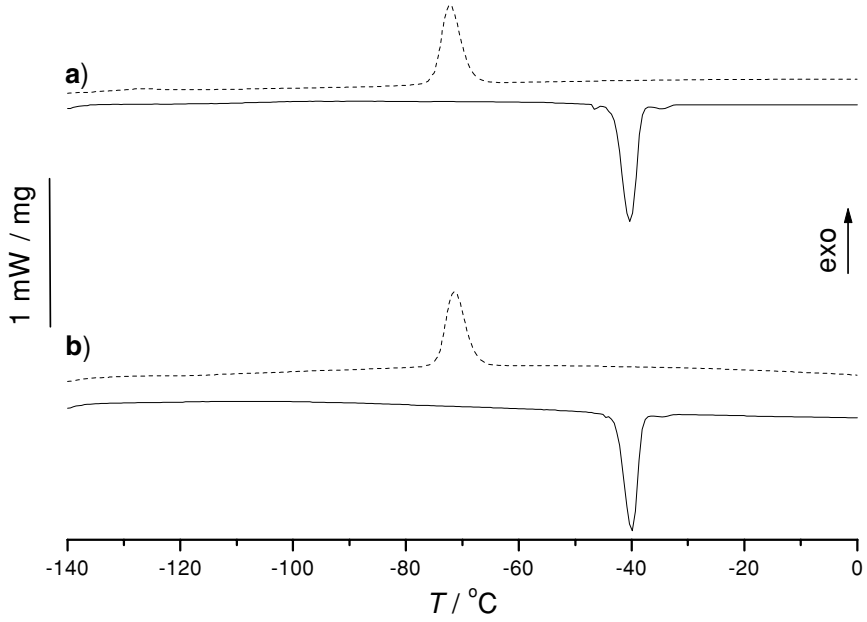

Figure 4. DSC thermograms of PDMS 15k filled with (a) 10 wt% dried M7D silica particles and (b) 10 wt% water-saturated M7D silica particles. Numerical values are specified in Table 2.

Table 2. Thermal data for the filled PDMS systems obtained by DSC at a cooling rate of -5 K min^{-1} and a heating rate of $+5$ K min^{-1}. Data are normalized with respect to the mass of PDMS.

	M7D dried	M7D water-saturated	M7D fluorinated	Hydrophilic CPG	Hydrophobic CPG
T_c	$-72.2°$C	$-71.4°$C	$-75.6°$C	$-72.3°$C	$-72.5°$C
ΔH_c	$+28.7$ J g^{-1}	$+27.5$ J g^{-1}	$+25.6$ J g^{-1}	$+26.6$ J g^{-1}	$+25.6$ J g^{-1}
T_m	$-40.3°$C; $-34.5°$C	$-40.0°$C	$-42.1°$C; $-33.6°$C	$-40.6°$C; $-33.5°$C	$-41.0°$C
ΔH_m	-28.1 J g^{-1}; -0.5 J g^{-1}	-30.0 J g^{-1}	-25.0 J g^{-1}; -2.4 J g^{-1}	-29.2 J g^{-1}; -6.8 J g^{-1}	-28.2 J g^{-1}

To examine the effect of sample preparation on the thermal behavior of the filled systems, a control experiment was performed. Pure PDMS was subjected to the preparation procedure used for the filled systems, without adding filler particles, and DSC curves were measured. No effect was observed when the thermograms of the resulting samples were compared to those of the untreated PDMS.

To test the effect of the cooling rate on the thermal features introduced above, a sequence of DSC experiments in which the cooling rate was varied from $\beta = -2$ K min^{-1} to a fast quench (in liquid nitrogen) was performed. Cooling was followed by a constant heating rate of $\beta = +5$ K min^{-1}. The resulting heating scans are presented in Fig. 5. We observe that crystallization takes place during cooling only at the two lowest cooling rates ($\beta = -2$ K min^{-1} and $\beta = -5$ K min^{-1}, Fig. 5(a) and (b)). Consequently, a loss of T_g and T_c during the heating scan is observed. This indicates that the high degree of crystallization was only achieved during the slow cooling process. The corresponding exotherm can readily be seen in the cooling curve (not given here). For a cooling rate of $\beta = -10$ K min^{-1} (Fig. 5(c)) a small T_g can be monitored and additionally a cold crystallization exotherm is observed in the heating scan. This implies that the crystallization process is partially quenched. For the quasi-infinite cooling rate (Fig. 5(d)) the heating curve resembles that of pure PDMS at intermediate cooling rates, i.e., the crystallization process is

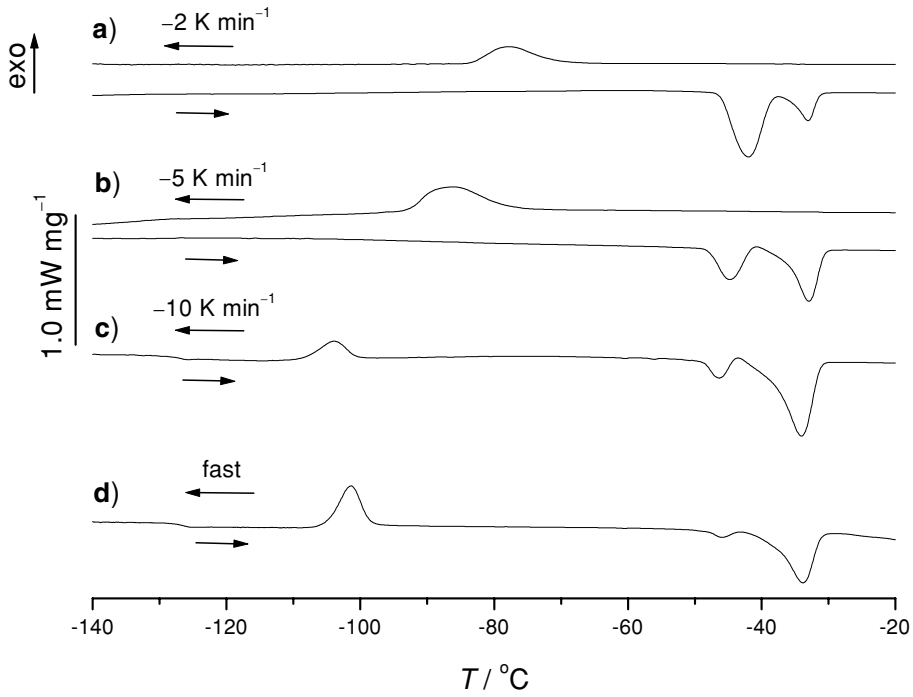

Figure 5. Heating scans of PDMS 16k filled with wt-10% water-saturated M7D silica particles. For the four scans the cooling rate, (a) -2 K min^{-1}, (b) -5 K min^{-1}, (c) -10 K min^{-1}, and (d) quasi-infinite (sample quenched in liquid nitrogen), prior to the heating curve was varied. The heating rate was always $+5$ K min^{-1}.

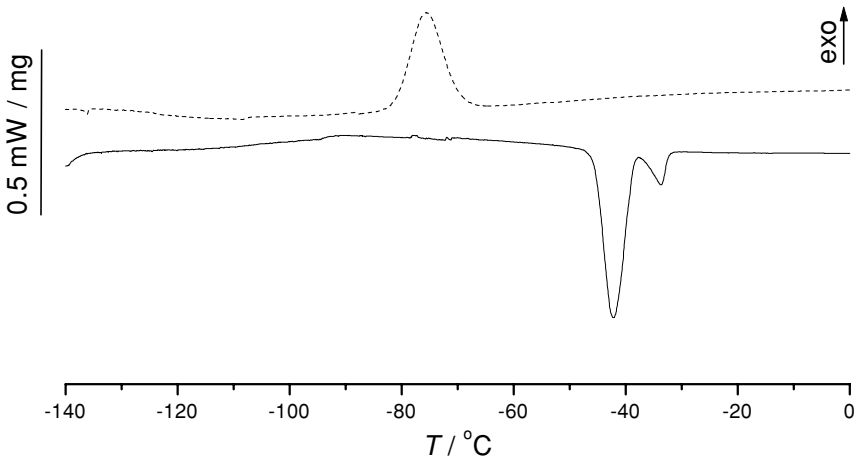

Figure 6. DSC thermogram of PDMS 15k + wt-10% fluorinated M7D silica particles. Numerical values are specified in Table 2.

basically quenched during the cooling cycle. Similar studies were carried out on pure PDMS. In contrast to the filled materials pure PDMS did not exhibit significant crystallization during the cooling cycle down to a cooling rate of $\beta = -2\,\mathrm{K\,min^{-1}}$. We note here that under isothermal conditions crystallization was observed at $T \leq -60^{\circ}$ C.

In Fig. 6 we present DSC thermograms of PDMS filled with fluorinated M7D silica particles. Data is given in Table 2. As previously mentioned, the PDMS melt does not wet the modified surface (contact angle of 45 ± 1). Yet, similar to the behavior presented in Fig. 5, an exothermic peak is found in the cooling curve, suggesting an enhanced tendency towards crystallization in the presence of the fluorinated additives as well. In this system subsequent cooling/heating cycles showed also similar behavior.

The studies described above were extended to the investigation of a different filler system, namely porous glass, CPG. The corresponding thermograms are given in Fig. 7 (and the data in Table 2). Both hydrophilic and hydrophobic CPG affected the crystallization behavior

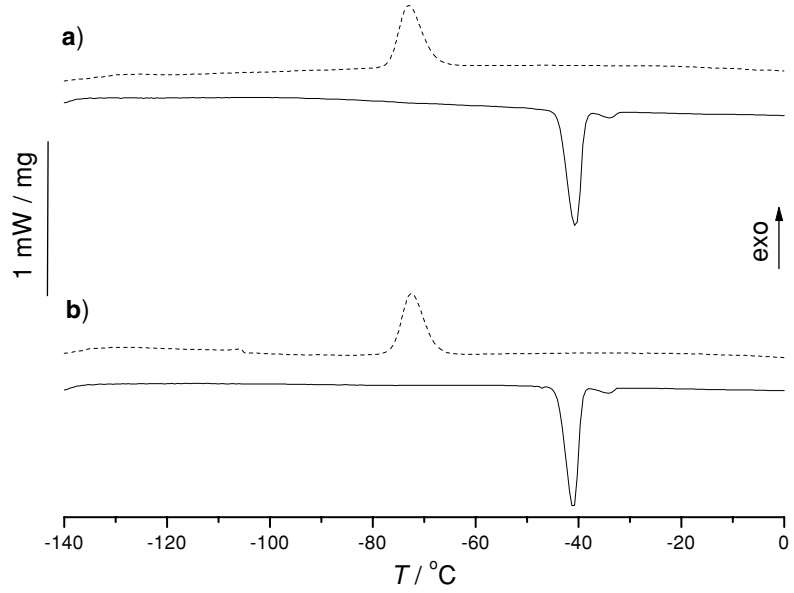

Figure 7. DSC thermograms of PDMS 15k filled with (a) wt-10% hydrophilic CPG and (b) wt-10% hydrophobic CPG. Numerical values are specified in Table 2.

of PDMS in a manner similar to that of the silica particles. In particular, at a given cooling rate the presence of either hydrophilic or hydrohobic CPG resulted in an enhanced crystallization rate, as indicated by the appearance of an exotherm in the cooling curve, and the disappearance of T_g and T_c in the heating curve.

4. Discussion

In this paper we describe an investigation of the effect of surfaces on the thermal behavior of a semicrystalline, practically non-entangled polymer melt. The model system is comprised of a low concentration of sub-micron particles or porous glass (CPG) embedded in the polymer melt. We find that, at a given cooling rate, solid additives regardless of their surface chemistry, enhance the crystallization rate of PDMS as measured in DSC experiments. The effect—within the range of our experiments—does not depend on the nature of the interactions between polymer chains and particle surfaces. In the following we discuss the observations and our interpretations starting from the pure PDMS system.

Thermal behavior of pure PDMS: The observed thermograms of pure PDMS are in agreement with previous observations [29–33]. In particular, the characteristic two-peak melting pattern (Fig. 3), typical of long chain polymers, is observed [34].

The effect of cooling rate: It is known that the cooling rate strongly affects the degree of crystallinity of semicrystalline materials [35, 36]. Crystallization is quenched by a fast cooling rate, leading to the formation of an amorphous glass while a slow cooling process enhances the crystallinity. According to models of polymer crystallization the actual crystallization rate, k_{cryst}, ($X^{-1}\mathrm{d}X/\mathrm{d}t$ where X is the crystal volume fraction), may be estimated by the following considerations: Polymer crystallization is possible within a temperature range bounded by an upper and a lower temperature. To allow for a certain degree of supercooling necessary for crystallization, the upper temperature has to be somewhat lower than the temperature at which the Gibbs free energy favors crystallization. The lower temperature is determined by the viscosity below which chain mobility (e.g., chain diffusion, prealignment, conformational changes) is hindered to the level preventing further chain rearrangements. Complete crystallization occurs in a DSC cooling experiment carried out at a rate, β, only if the crystallization rate fulfills $k_{\text{cryst}} \gg \beta \cdot \Delta T^{-1}$. Here ΔT is the difference between the two critical crystallization temperatures. One may obtain the upper critical crystallization temperature from the onset of the crystallization exotherm and the lower critical temperature from the onset of the cold-crystallization process in a heating-scan performed at the same rate of temperature change. In our case we find a ΔT of 30 K. For the given cooling rate of $\beta = -5\ \mathrm{K\ min^{-1}}$ the material has 6 min to complete the crystallization process. For pure PDMS this cooling rate is apparently too fast. The crystallization rate has been estimated from isothermal experiments and found to be $k_{\text{cryst}} < 0.003\ \mathrm{s^{-1}}$. Our observations indicate that filled PDMS readily crystallizes under these conditions and hence, $k_{\text{cryst}} > 0.003\ \mathrm{s^{-1}}$. PDMS turns out to be a particularly suitable polymer for the investigation of cooling rates via DSC experiments, probably due to its exceptionally high flexibility combined with the low crystallization temperature [37].

Surface effects: Different types of surfaces exhibiting a range of interfacial energies, were investigated. We studied the effect of "attractive surfaces" such as non-coated silica particles (Fig. 4) and hydrophilic CPG (Fig. 7(a)) that are known to adsorb PDMS from the melt, probably due to their silanol surface groups [25]. "Non-attractive" surfaces that are not wetted by and do not adsorb PDMS from the melt, such as the fluorinated silica particles, water-saturated particles, and hydrophobic CPG were investigated as well. The key observation of the present study is that independently of the surface chemistry, the very presence of the surfaces enhances the crystallization rate of PDMS.

The effect of filler particles on the thermal behavior of PDMS was investigated extensively before [22, 39–41]. In some of these studies it was found that filler particles enhanced crystallization, and the results were interpreted as evidence for heterogeneous nucleation. In other studies it was concluded that the presence of solid particles does not affect the crystallization [39], and in others that the degree of crystallinity is reduced [40]. In some of these studies, however, the samples were prepared in a way as to remove non-adsorbed polymers so that only a surface layer of adsorbed polymers was present [41]. In other experiments the samples were quenched into the solid phase, rather than cooled slowly. As was discussed above, and observed in this study (Fig. 5), a fast quench leads to vitrification of the melt and dominates over the tendency of solid additives to induce crystallinity.

Although these phenomena are experimentally particularly easy to address using PDMS samples, we

believe that our observations are not unique to PDMS and should be considered for semicrystalline polymers in general. In the systems studied here, entropic effects obviously predominate. This, however, will not always be the case. Indeed, as was suggested by Cabane and coworkers a highly crystallizable polymer such as polyethylene oxide, PEO, may be affected differently by the presence of additives [42]. Depending on the chemistry involved, the balance of enthalpic and entropic effects may be different for different semicrystalline materials.

The fact that our results are deduced from DSC measurements suggests that the effects are non-local and result in a surface-induced bulk crystallization. In Fig. 2 we presented the TEM image of M7D particles embedded in a PDMS melt. In these samples, the inter-particle distance is of the order of a micron (10 wt% filler content). It is therefore evident that the inter-particle regions constitute a significant fraction of the sample.

Relation to models of crystallization: In the classical models such as that by Lauritzen and Hoffman [14] a description of spherulitic growth rate G (cm s^{-1}) is given by the expression:

$$G = G_0 \exp\left(-\frac{U^*}{R(T - T_0)}\right) \exp\left(-\frac{K_g}{T(T - T_m)}\right)$$

where T is the isothermal crystallization temperature, G_0 takes into account the geometric parameters of both the polymer chain and the crystalline lamella. U^* denotes the free energy of activation that governs the rate of chain segments transport to the growth front, with a temperature dependence similar to that of the viscosity. K_g is a nucleation constant, and $T - T_m$ the degree of under-cooling. In general, for this type of temperature dependence, the rate of crystallization passes through a maximum, as the temperature increases from the glass transition temperature (where U^* becomes infinite) to the vicinity of the melting temperature, where $T - T_m = 0$.

The crystallization rates, as deduced from the DSC measurements presented here, are consistent with the predicted acceleration of the crystallization rate with temperature reduction (in the range between the melting point and the glass-transition temperature), as indicated by the cold crystallization (for example, Fig. 2). At the same time, the accelerated rate of crystallization of the filled materials, as deduced from the DSC measurements, is not consistent with other aspects of the kinetic equation: The filled PDMS is characterized by a significantly higher viscosity than that of the native material. A higher viscosity of the crystallizing material should decrease the mobility, and therefore should have caused a reduction of the crystallization rate, unlike the observations. In addition, we recall that in some of the systems PDMS does not wet the particles, so in the framework of the classical theories of nucleation, we do not expect the particles to serve as efficient centers for epitaxial crystallization, or sites for heterogeneous nucleation.

The role of entropy: The observations may be rationalized by realizing the important role of entropy in polymer-surface interactions. It is known that surfaces act as a strong perturbation to the melt, and may modify the free energy landscape of the system. Two of the specific mechanisms by which entropic interactions act, are enrichment of chain ends at the vicinity of the surface [43], and the enhancement of orientational ordering of polymeric coils due to the presence of a surface [44–48]. Indeed, filler-induced deformation of polymer chains has recently been detected by small-angle neutron scattering (SANS) in polysilicate filled PDMS [49]. When the chain dimensions were approximately the same magnitude as the filler particle diameters, the scattering results showed a decrease in the radius of gyration, R_g for all filler concentrations. For longer chains and low filler concentration an increase in chain dimension was observed, in semi-quantitative agreement with the results of Monte Carlo simulations [50]. In our study, the filler particles are much larger in diameter than the coil dimensions with R_g in the range of 3.5 nm [49]. However, a recent molecular dynamic computer simulation by Starr et al. [47] suggested that in the vicinity of a surface (either attractive or non-attractive) polymer coils become slightly elongated and significantly flattened.

Local ordering at the molecular level as result of the hindered dynamics, was recently observed by solid-state NMR measurements. At temperatures between $T_g + 50$ K and $T_g + 150$ K it was demonstrated that on time scales of a few tens of milliseconds up to the terminal relaxation time, polymer melts that experience other types of constraints such as entanglements [50] exhibit substantial long-lived ordering, which increase in the presence of confinement such as rigid blocks in block copolymers [51].

The experimental and theoretical results described in these studies were concerned with amorphous polymers and are related to the effect of surfaces on the glass-transition temperature. Yet, we believe that

similar effects, of pure entropic nature, are important for crystallization: In line with the experimental observations presented in this work, we suggest that regions of non-random chain conformations on intermediate length scales [52] may play an important role in the early stages of crystallization, even if the orientational ordering of these regions does not match that of the lowest energy crystalline phase. These regions may offer a different pathway for crystallization by allowing the system to bypass kinetic barriers that delay crystallization in a native melt.

Finally, we address the issue of adsorbing surfaces. In this case short range interactions (hydrogen bonding in our system) lead to adsorption of a polymeric monolayer. The solid/melt interface is replaced by a surface coated by a fluffy polymeric layer resulting in entropic repulsion at the interface between the melt and the adsorbed layer. This type of interaction is consistent with the effect of the non-adsorbing surfaces.

5. Summary and Conclusions

To summarize, we found that particles and porous glass with a high surface area and different types of surface interactions accelerate the crystallization rate of non-entangled PDMS melts, as observed in DSC experiments. The effect does not depend on the specific type of interfacial interaction between the additives and the polymer, but is rather affected by the presence of a surface. We suggest that the origins of the effect are entropic, i.e. the conformational space of the chains is modified by the presence of the surface. The mechanism how this change affects crystallization and in particular the role of chain ends and/or the distortion of the chain dimensions in boundary layers remains to be clarified in the future.

Acknowledgments

We would like to thank Profs. J. Baschnagel, G. Strobl, B. Cabane, and I. Szleifer for illuminating discussions, and Prof. Y. Cohen for his remarks. We also thank Mettler Toledo, and especially Dr. R. Riesen for discussing instrumental aspects with us. We would like to express our gratitude to T. Wagner for synthesizing the PDMS 16K. TD acknowledges a fellowship from the MINERVA foundation. This work was funded through the Infrastructure Research Program of the Israel Ministry of Science and Culture (grant no. 8625), and the United States-Israel Binational Science Foundation (BSF 2000124).

Notes

1. This idea is utilized in industrial processing of polymers such poly (ethylene terephthalate) PET, poly (vinyldene fluoride) (PVDF), and Nylon. During the fiber spinning process crystalline fibers are formed by extrusion of the melt through a set of small circular dies, drawing and fast cooling. The pre-ordered melt forms upon cooling highly crystalline materials.
2. We note that the M_e for PDMS as determined from dynamic mechanical analysis is usually reported to be in the range between 11,300 and 16,600 g mol^{-1} depending on the evaluation details. Since quite a few entanglements per chain are required to yield an observable entanglement effect, the PDMS 16k can be regarded as non-entangled material [38].

References

1. Y. Cohen and S. Reich, Journal of Polymer Science **19**, 599 (1981).
2. N.K. Dutta, N.R. Choudhury, B. Haidar, A. Vidal, J.B. Donnet, L. Delmotte, and J.M. Chezeau, Polymer **35**, 4293 (1994).
3. K.U. Kirst, F. Kremer, and V.M. Litvinov, Macromolecules **26**, 975 (1993).
4. X. Zheng et al., Phys. Rev. Lett. **74**, 407 (1995).
5. V. Arrighi, J.S. Higgins, A.N. Burgess, and G. Floudas, Polymer **39**, 6369 (1998).
6. E.K. Lin, R. Kolb, S.K Satija, and W.L. Wu, Macromolecules **32**, 3753 (1999).
7. V.J. Novotny, J. Chem. Phys. **92**, 3189 (1990).
8. J.L. Keddie, R.A.L. Jones, and R.A. Cory, Europhys. Lett. **27**, 59 (1994).
9. J.L. Keddie, R.A.L. Jones, and R.A. Cory, Faraday Discuss. **98**, 219 (1994).
10. G. Tsagaropoulos and A. Eisenberg, Macromolecules **28**, 6067 (1995).
11. J.A. Forrest, K. Dalnoki-Veress, J.R. Stevens, and J.R. Dutcher, Phys. Rev. Lett. **77**, 2002 (1996).
12. G. Strobl, *The Physics of Polymers*, 2nd ed. (Springer-Verlag, Berlin, 1997).
13. J. Jancar (ed.), Structure-Property Relationships in Thermoplastic Matrices, Adv. Polym. Sci. **139**, 1 (1999).
14. J.D. Hoffman, G.T. Davis, and J.I. Lauritzen, in *Treatise on Solid State Chemistry*, Vol. 3, edited by N.B. Hannay (Plenum Press, 1976), p. 497.
15. L. Mandelkern, in *Crystallization of Polymers* (McGraw Hill, New York, 1994).
16. B. Wunderlich, in *Crystal Nucleation, Growth, Annealing*, Macromolecular Physics, Vol. 2 (Academic Press, New York, 1976).
17. J.D. Hoffman, R.L. Miller, H. Marand, and D.B. Roitman, Macromolecules **25**, 2221 (1992).
18. D.M. Sadler, Nature **326**, 174 (1987).
19. B. Heck, T. Hugel, M. Iijima, and G. Strobl, Polymer **41**, 8839 (2000).
20. G. Strobl, Eur. Phys. J. **E 3**, 165 (2000).

21. K. Zahn, R. Lenke, and G. Maret, Phys. Rev. Lett. **82**, 2721 (1999).
22. E.B. Sirota, Langmuir **14**, 3133 (1998).
23. M.I. Aranguren, Polymer **39**, 4897 (1998).
24. T. Dollase, H.W. Spiess, M. Gottlieb, and R. Yerushalmi-Rozen, Europhysics Letters **60**(3), 390 (2002).
25. W. Haller, J. Am. Ceram. Soc. **57**, 120 (1974).
26. R.K. Iler, *The Chemistry of Silica* (Wiley, New York, 1979).
27. W.W. Wendlandt and P.K. Gallagher, *Thermal Characterization of Polymeric Materials*, edited by E.A. Turi, 2nd ed. (Academic Press, San Diego, 1997).
28. V.B.F. Mathod (ed.), *Calorimetry and Thermal Analysis of Polymers* (C. Hanser, Munich, 1994).
29. A. Yim and L.E.St. Pierre, J. Polym. Sci. Polym. Lett. **8**, 241 (1970).
30. B. Ke, J. Polym. Sci. Polym. Lett. **1**, 167 (1963).
31. C.L. Lee, O.K. Johannson, O.L. Flaningam, and P. Hahn, ACS Polym. Prepr. **10**, 1313 (1969).
32. J.D. Helmer and K.E. Polmanteer, J. Appl. Polym. Sci. **13**, 2113 (1969).
33. J.S. Clarson, K. Dodgson, and J.A. Semlyen, Polymer **26**, 930 (1985).
34. S.L. Liu, T.S. Chung, H. Oikawa, and A. Yamaguchi, Journal of Polymer Science: Part B: Polymer Physics, **38**, 3018 (2000).
35. R. Androsch and B. Wunderlich, Macromolecules **33**, 9076 (2000).
36. K. Armistead and G. Goldbeck-Wood, Adv. Polym. Sci. **100**, 219 (1992).
37. P.C. Hiemenz, *Polymer Chemistry* (Marcel Dekker Inc., New York and Basel, 1984).
38. J.D. Ferry, *Viscoelastic Properties of Polymers*, 3rd ed. (Wiley, New York, 1980).
39. J.E. Mark, J.M. Zeigler, and F.W.G. Fearon (eds.), *Silicon-based Polymer Science* (ACS, Washington, 1990).
40. A. Voeit, J. Polym. Sci. Macromol. Rev. **15**, 327 (1980).
41. Y.S. Lipatov and F.G. Fabulyak, Vysokomol. Soyed A **10**, 1605 (1968).
42. R.H. Ebengou and J.P. Cohen-Addad, Polymer **35**, 14 (1994).
43. B. Cabane, private communication.
44. D.T. Wu, G.H. Fredrickson, J.P. Carton, A. Ajdari, and L. Leibler, J Polymer Science: Part B: Polymer Physics **33**, 2373 (1995).
45. J.H. van Vliet and G. ten Brinke, J. Chem. Phys. **93**, 1436 (1990).
46. J. Baschnagel and K. Binder, Macromolecules **28**, 6808 (1995).
47. K. Binder, A. Milchev, and J. Baschnagel, Annu. Rev. Mat. Sci. **26**, 107 (1996).
48. F.W. Starr, T.B. Schroder, and S.C. Glotzer, Phys. Rev. E. **64**, (2001).
49. M.A. Sharaf and J.E. Mark, Polymer **43**, 643 (2002).
50. A.I. Nakatami, W. Chen, R.G. Schmidt, G.V. Gordon, and C.C. Han, Polymer **42**, 3713 (2001).
51. R. Graf, A. Heuer, and H.W. Spiess, Phys. Rev. Lett. **80**, 5738 (1998).
52. T. Dollase, R. Graf, A. Heuer, and H.W. Spiess, Macromolecules **34**, 298 (2001).